Transdermal Macromolecular Delivery: Real-Time Visualization of Iontophoretic and Chemically Enhanced Transport Using Two-Photon Excitation Microscopy

Burrinder S. Grewal,[1,3] Aarti Naik,[2] William J. Irwin,[1,5] Gert Gooris,[3] Cees J. de Grauw,[4] Hans G. Gerritsen,[4] and Joke A. Bouwstra[3]

Received March 1, 2000; accepted April 11, 2000

Purpose. To investigate the transdermal delivery of a model macromolecule by passive and iontophoretic means following pretreatment with C_{12}-penetration enhancers and to visualise transport across human stratum corneum (SC) in real time.

Methods. Transport studies of dextran, labelled with fluorescent Cascade Blue® (D-CB; M_R = 3 kDa) across human stratum corneum, were conducted during passive and iontophoretic modes of delivery following pretreatment with either dodecyltrimethylammonium bromide (DTAB), sodium dodecyl sulphate (SDS) or Azone®. Size-exclusion chromatography was used to assess maintenance of dextran structural integrity throughout experimental lifetime. Two-photon excitation microscopy was employed to visualise real-time dextran transport during current application.

Results. The positively charged C_{12}-enhancer DTAB elevated passive D-CB steady-state flux (J_{ss}) and was the only enhancer to do so above control during iontophoresis. The negatively charged SDS had the least effect during both stages. On-line macromolecular transport was visualised, indicating both inter- and intra-cellular pathways across SC during current application. No transport was visible across untreated SC during passive transport.

Conclusions. Use of a positively charged enhancer may improve J_{ss} of anionic macromolecular penetrants during passive and iontophoretic delivery. On-line visualisation of iontophoresis across SC was possible and can provide mechanistic insight into SC transport pathways.

KEY WORDS: dextran; iontophoresis; stratum corneum; transdermal enhancers; transport pathways; two-photon excitation microscopy.

[1] Pharmaceutical Sciences Research Institute, Aston Pharmacy School, Aston University, Birmingham, B4 7ET, UK.

[2] Centre Interuniversitaire de Recherche et d'Enseignement, Archamps, France.

[3] Leiden/Amsterdam Centre for Drug Research, Gorlaeus Laboratories, Leiden University, The Netherlands.

[4] Debye Institute, Department of Molecular Biophysics, Utrecht University, The Netherlands.

[5] To whom correspondence should be addressed. (e-mail: w.j.irwin@aston.ac.uk)

ABBREVIATIONS CB, Cascade Blue®; D-CB, dextran-Cascade Blue®; DTAB, dodecyltrimethylammonium bromide; epi, epidermis (split-thickness skin); J_{SS}, steady-state flux; LSCM, laser scanning confocal microscopy; PBS, phosphate-buffered saline; PG, propylene glycol; SC, stratum corneum; SDS, sodium dodecyl sulphate; SEC, size-exclusion chromatography; TPEM, two-photon excitation microscopy.

INTRODUCTION

Transdermal iontophoresis and the use of percutaneous penetration enhancers are physical and chemical means to improve the delivery of applied drugs through skin. Both methods aim to reversibly perturb the naturally occurring barrier function of the SC. Transdermal iontophoresis is an electrically assisted means of delivering both charged and uncharged molecules. In essence, charged molecules are brought into contact with skin and a driver electrode of similar polarity. The circuit is completed by connecting this electrode to one of opposite charge which is likewise placed in an electrolyte solution also in contact with skin. When an electromotive force is applied, electro-repulsion occurs at the driving electrode surface, serving to propel the drug into the adjacent skin. The use of chemical enhancers to ease the diffusion or partition of drugs into stratum corneum has been well documented and many different groups of percutaneous enhancers have now been identified (1–3). Under passive diffusion, the mechanisms of action of such chemicals are commonly separated under two distinct headings; those that increase solute solubility, in stratum corneum (4) and those that perturb its compact structure, perhaps by creating enhancer-rich domains which result in an increase in permeant diffusion coefficient (3,5). What is less clear, however, is the mechanism of chemical-enhancer action in conjunction with iontophoresis; early reports suggest that the charge which an enhancer carries is important (6,7) while some studies have reported no significant additive affect (8,9).

Both methods of enhancement have been employed separately over many years to optimise the transdermal delivery of a multitude of therapeutic entities; efforts so far generally having been concentrated towards solutes having a molecular weight of less than 1000 Da (10). It is well accepted that, for iontophoretic and chemical modes of enhancement, an inverse relationship exists between drug flux and permeant molecular weight (11,12). However, the challenge to deliver effectively into the body the new generation of biotechnologically produced drugs (13) is, amongst other factors, intrinsically linked to their comparatively large molecular weights (11,12). The objectives of this study were to combine iontophoresis and the use of enhancers in an attempt to assess transdermal flux of a model macromolecular compound, dextran (M_R 3 kDa), and to investigate the prevalent mechanisms of enhancement. The dextran (D) used in experiments carried three negative charges by virtue of coupling to the fluorescent probe, Cascade Blue® (CB). Electrically assisted and passive diffusional profiles, together with steady-state flux values, have been determined and contrasted. Further, this paper describes the real-time visualisation of iontophoretically driven D-CB across human skin in order to determine macromolecular transport pathways. To date, most studies have used laser-scanning confocal microscopy (LSCM) to visualise iontophoretic transport resulting from current application (14). Recent visualisation studies by Turner *et al.* (15,16) have used LSCM and reported on the relationship between penetrant physicochemical properties and current-mediated transport in skin. Here, we report findings from visualisation studies carried out on-line during current application employing scanning two-photon excitation microscopy (TPEM). TPEM (with wide-field detection) has distinct advantages over the more routine LSCM (single photon) when used to image skin

0724-8741/00/0700-0788$18.00/0

(17); light-scattering by the stratum corneum is reduced, resulting in greater image contrast and depth of penetration. Outside the focal area, absorption is negligible and autofluorescence, which is generally in the blue-violet region of the spectrum is reduced. This results in less photobleaching (18) and less photodamage to the sample. Although the peak intensity with two-photon excitation is high (high temporal intensity) in the focal region, the time-averaged power is comparatively low - usually in the order of milliwatts. These powers have no effect on the vitality of cells (19).

MATERIALS AND METHODS

Materials

Dextran-labelled with Cascade Blue® (D-CB) of molecular weight 3 kDa and free-label Cascade Blue® were purchased from Molecular Probes (Leiden, Holland). All enhancers (apart from Azone®) and propylene glycol were obtained from Sigma Chemicals (St. Louis, USA). Azone® was a gift from Whitby Research Ltd. The buffer used was phosphate-buffered saline (PBS) pH 7.4 (8 mM Na_2HPO_4, 1.5 mM KH_2PO_4, 139 mM NaCl, 2.5 mM KCl in double-distilled, filtered water). Solutions of D-CB were prepared in PBS. Ag and AgCl electrodes were prepared and regenerated as described by Geddes *et al.* (20). All silver products were purchased from Aldrich (Barnem, Belgium).

Epidermis and Stratum Corneum Preparation

Whole thickness abdominal skin was obtained from local hospitals following cosmetic surgery; the underlying subcutaneous fat was removed using a surgical scalpel and the skin was then dermatomed to a thickness of 200 μm (Padgett Electro Dermatome Model B, Kansas City, USA). The epidermal sheet was spread flat on filter paper soaked in 0.1% trypsin solution (Type III from bovine pancreas, Sigma Chemicals, St. Louis, USA) and stored in a refrigerator at 4°C overnight. The following day, the skin was removed and placed in a oven at 37°C for one hour after which the SC was carefully teased away from the remaining underlying epidermis. Each SC sheet was then washed in an aqueous 0.1% trypsin inhibitor solution (Type II from soybean, Sigma Chemicals, St. Louis, USA) by gentle shaking for 30 seconds. Sheets of SC were subsequently rinsed twice in double-distilled, filtered water, transferred to wire gauze, left to dry at room temperature and finally stored over silica gel in a nitrogen-rich and air-tight atmosphere until needed for experiments.

Iontophoresis Experiments

Pretreatment with Enhancers

SC sheets were floated on double-distilled, filtered (0.54 μm) water—the dermal side being in contact with water—and left to hydrate for two hours. Dialysis tubing membrane having a molecular weight cut off of 50,000 Da (Hicol bv, Holland) was immersed in a beaker of water containing 1% $NaHCO_3$ (Sigma, UK), boiled for 30 minutes, allowed to cool and washed in water. Using a steel punch and die, circular discs (13 mm) were cut out from SC and membrane, and each piece of SC was carefully positioned on a dialysis membrane disc to provide support for the tissue. Two pieces of SC were then sandwiched in each of the three compartmental iontophoretic cells as previously described (21). PBS was pipetted into cell-acceptor compartments to prevent dehydration of the SC and 120 μl of enhancer solution (0.16 M in PG) pipetted into the cathodal (donor) chamber ensuring that the entire SC surface was covered. The cells were left positioned vertically for 18 hours after which the SC was washed three times with PBS to remove any traces of enhancer.

Transport Studies

Transport experiments, to determine steady-state flux as a function of donor concentration and enhancer pretreatment, were performed. PBS and D-CB (0.10–0.2 mM) solutions (2 ml) were pipetted into the receptor and donor compartments and Ag (anode) and AgCl (cathode) electrodes were inserted into these chambers respectively. The electrodes were connected to a 6-channel computer-controlled current source powered by a 40 volt supply (Electronic Department, Leiden University). Anodal and cathodal chambers were continuously stirred at 375 rpm. PBS was continuously pumped at a rate of 7 ml h^{-1} through the central acceptor compartment (volume 0.5 ml) from a reservoir to a Retriever IV fraction collector (Isco, Holland) using a peristaltic pump (Ismatec SA, Switzerland). Fractions were collected hourly in test tubes and then assayed for dextran content. Each experiment started with a six-hour passive period (no current) and was followed by nine hours of current application (500 μA cm^{-2}) and finally a six-hour passive post-iontophoretic period without current. Dextran concentrations were determined by measuring fluorescence intensity on a Jasco 821-FP (H. I. Ambacht, Holland) detector (Ex 401, Em 431 nm) connected to an autosampler (Gilson 234 autoinjector, UK.) using PBS as the mobile phase at a flow rate of 0.5 ml min^{-1}. A linear relationship existed over the range 7.5–100 ng ml^{-1} ($r^2 = 0.99$, data not shown). Flux *versus* time profiles were then produced. Relevant transport studies involving the use of free label Cascade® Blue in PBS (0.1 mM) were also performed following an identical methodology.

Size-Exclusion Chromatography (SEC)

To determine the integrity of D-CB in the presence and absence of electrical current, SEC analysis was performed. Samples of solution were taken from all cell compartments during all stages of transport studies. Each sample was then injected into a 8 × 300 mm Suprema 30 SEC column (Polymer Standards Service, Germany) having a particle diameter of 10 μm. The column was attached to a Isochrom solvent-pump (Spectra-Physics, England, flow rate: 1 ml min^{-1}) and a fluorescence detector (Jasco 821-FP, H. I. Ambacht, Holland). The excitation and emission wavelengths were 401 nm and 431 nm respectively. The mobile phase was PBS. The retention time for all peaks was between 7 and 10 minutes.

Two-Photon Excitation Microscopic Visualisation of Transport

A two-photon excitation microscope employing a mode-locked titanium:sapphire laser as the light source (Tsunami, Spectra Physics) was used to image transport. The microscope

is described fully elsewhere (17). Human epidermis (split-thickness skin) having a thickness of 200 μm was used either untreated or pretreated with DTAB in the same manner as described above for SC. Fresh skin samples were mounted in a specially designed cell bringing the skin surface into contact with the 0.1 mM D-CB solution and allowing both the application of current (500 μA cm^{-2}) across electrodes and penetration of the laser (excitation wavelength 800 nm, average laser power 3 mW) into the skin. XY images having dimensions of 95 × 95 μm (256 × 256 pixels) were collected at regular time intervals at 10, 15 and 20 microns deep into the SC during passive and electrically enhanced (500 μA cm^{-2}) periods of delivery. XZ images were also compiled. The minimal time-resolution was approximately 4 minutes using a 60× NAI.2 objective which resulted in an imaging resolution of 0.27 μm and 0.72 μm in XY (lateral optical resolution) and XZ (axial optical resolution) planes respectively (22).

Statistical Analysis

All transport cell results are represented as the means of 4 to 11 experiments ± standard errors. Statistical difference was tested for by using an unpaired Student's t-test, statistical significance being defined as $p < 0.05$.

RESULTS AND DISCUSSION

Untreated Stratum Corneum

The dependence of dextran transport on donor concentration is illustrated in Fig. 1 which summarises steady-state flux (J_{ss}) values for Cascade Blue®-labelled dextran (D-CB), as a function of donor concentration and treatment regimen (stage 1: 6 hours of passive transport; stage 2: 9 hours of iontophoresis; and stage 3: 6 hours of passive delivery). The corresponding permeation profile for an applied D-CB concentration of 0.1 mM is shown in Fig. 2. Dextran transport was not detected during stage 1 but was significantly enhanced during, and subsequent to, the application of an electrical potential (stages 2 and 3, respectively). On application of current (500 μA cm^{-2}), an immediate increase in D-CB flux was observed, with iontophoretic fluxes reaching steady state within 5 hours and being linearly proportional to the applied drug concentration ($r^2 = 0.99$). Typically (23), J_{ss} at six-hours post-iontophoresis did not return to passive pre-iontophoretic levels, but ranged between 8–10% of that during iontophoresis which may indicate possible current- or water-induced perturbation of SC permeability (see also Table I).

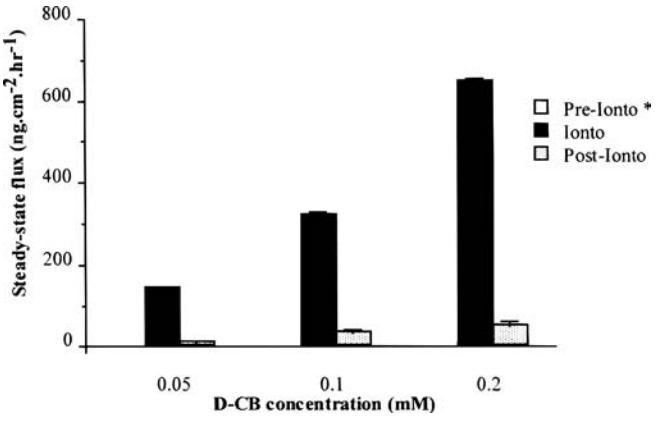

Fig. 1. Effect of D-CB donor concentration on permeant steady-state flux across untreated human stratum corneum. *Note: pre-iontophoretic (i.e., passive) D-CB transport was below the limit of detection.

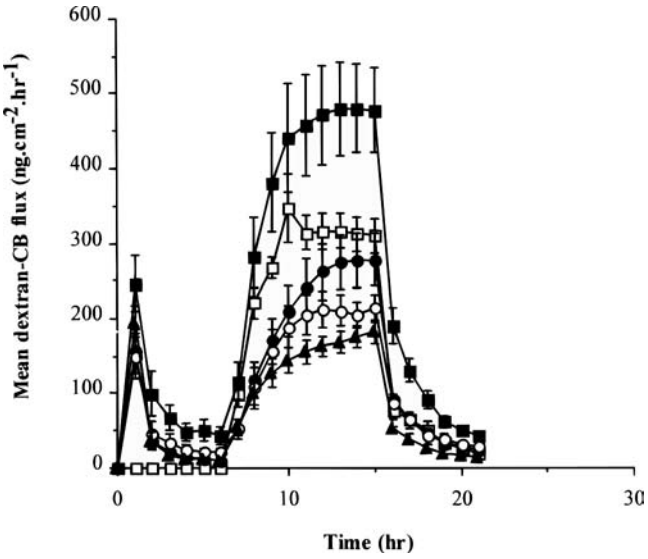

Fig. 2. Passive and iontophoretic permeation profiles of D-CB (0.1 mM) across human stratum corneum. —□—, untreated SC; —■—, pretreatment with 0.16 M DTAB/PG; —●—, pretreatment with neat propylene glycol; —○—, pretreatment with 0.16 M Azone® in PG; and —▲—, pretreatment with 0.16 M SDS in PG. Current was applied for nine hours between t = 6 and t = 15 h.

Pre-Iontophoresis

To assess enhancer effects on dextran transport, SC was pretreated with either a cationic (DTAB), anionic (SDS) or

Table I. Steady-State Flux for Dextran-Cascade Blue® (D-CB) and Free Cascade Blue® (CB) Transport Dependent Upon Chemical Pretreatment During Passive and/or Iontophoretic Modes of Delivery

	Steady-state flux (ng cm^{-2} h^{-1})		
Enhancer Pretreatment	Pre-iontophoresis (Stage 1)	Iontophoresis (Stage 2)	Post-iontophoresis (Stage 3)
No Pretreatment			
D-CB	nd	313.7 ± 10.9	26.5 ± 4.9
CB	nd	703.6 ± 21.3	27.3 ± 3.0
PG only			
D-CB	11.8 ± 2.6	272.7 ± 17.0	28.8 ± 2.1
CB	30.9 ± 7.7	950.9 ± 54.2	79.1 ± 14.7
Azone®			
D-CB	22.7 ± 3.1	210.3 ± 9.6	33.6 ± 2.2
CB	27.7 ± 1.3	589.8 ± 6.7	47.1 ± 1.7
DTAB			
D-CB	47.5 ± 7.2	477.2 ± 29.3	52.2 ± 3.1
SDS			
D-CB	11.5 ± 1.7	172.7 ± 7.0	17.2 ± 1.5

Note: nd, not detectable.

uncharged (Azone®) transdermal penetration enhancer (0.16 M) in PG. The concentration of Azone (0.16 M) was chosen as studies (24) have shown that, at this concentration, Azone is able to perturb rigid skin lipid domains which can be correlated with increased permeability of the tissue. The other enhancers were applied to skin at the same concentration. An *in vivo* study (25), where Azone and surfactants were applied to human skin in very similar concentrations, reported no adverse toxicological affects. Figure 2 profiles dextran diffusion across SC from a 0.1 mM D-CB donor solution as a function of the pretreatment employed. The first phase (t = 0–6 h) represents passive diffusion; this is followed by 9 hours of iontophoresis, after which current application is terminated with post-iontophoretic, passive diffusion being monitored for a further 6 hours. D-CB steady-state values (or the mean of the last three points for SDS), as a function of enhancer pretreatment and delivery protocol are summarised in Table I. During stage 1, all systems (including PG used as the vehicle) significantly elevated passive D-CB flux relative to that of untreated SC. When compared to the PG-treated control (to differentiate between vehicle and enhancer effect), the greatest degree of passive enhancement was achieved by DTAB (4-fold), followed by Azone® (2-fold), while the activity of SDS was equivalent to that of the solvent, PG (Fig. 3). Interestingly, flux measurements recorded during the first hour of stage 1 showed an unexpected spike for each enhancer-mediated profile (Fig. 2). An explanation could be enhancer washout from SC during the first hour of permeation; this might have reduced enhancer effects and invalidated comparisons of enhancer performance, derived from D-CB steady-state flux determinations, during iontophoresis. In order to resolve this issue, experiments which excluded stage 1, thereby ruling out any possibility of passive enhancer washout from the SC, but comprising stages 2 and 3, following DTAB pretreatment, were conducted. The steady-state flux produced under these conditions was not significantly different ($P > 0.05$) from that obtained earlier (Table I under stage 2). Thus, the spike is probably not caused by enhancer washout during stage 1 and its occurrence did not affect chemically enhanced iontophoretic steady-state flux. Although the cause of this spike remains unknown, the observation that this peak is absent in untreated skin but present in all PG-treated samples (including PG alone) suggests it is solvent-mediated.

Passive transport was visualised using TPEM. Figure 4 shows two xy images, taken by the TPE microscope, of human SC at a depth of 10 microns (before the onset of current) and after 60 minutes passive D-CB diffusion from a 0.1 mM donor solution. Image (a) is of an untreated sample whilst image (b) is of a sample pretreated for 16 hours with 0.16 M DTAB/PG, the most effective penetration enhancer in this study. Skin corneocytes and intercellular domains are clearly highlighted by the distribution of D-CB (Fig. 4b), whilst some intracellular accumulation is also evident in the treated sample. However, there is no apparent transport or absorption of D-CB occurring in the untreated sample (Fig. 4a). These findings are similar to those previously reported for calcein at a depth of 10 μm in mouse SC (15) and also parallel the findings of our diffusion studies from which demonstrated an absence of passive transport in untreated skin (Fig. 2).

The DTAB-mediated flux of D-CB was 4-fold greater than that observed with SDS. This is consistent with literature reports of greater enhancing effects attributable to cationic rather than anionic surfactants (26). In comparison, SC pretreated with Azone® exhibited J_{ss} above that of SDS but lower than DTAB. Previously, it has been shown to enhance the flux of a variety of macromolecules (27). All enhancers used share a common C_{12}-alkyl chain but possess a headgroup that varies in polarity—it is likely that this affects the negative charge of the skin (28) and modulates the flux of anionic D-CB. Thus, cationic DTAB may lower SC negativity, reducing electrostatic repulsion between similarly charged SC and D-CB to enhance flux. In contrast, SDS could magnify surface negative charge and enhance repulsion between membrane and permeant.

Iontophoresis

In contrast to an undetectable passive flux, iontophoresis provided a steady-state flux for D-CB of 313.7 ± 10.9 ng cm^{-2} h^{-1} after ~6 h of current application (Fig. 2/3, Table I). When an iontophoretic current was applied following chemical pretreatment of SC, to drive D-CB across the membrane, the

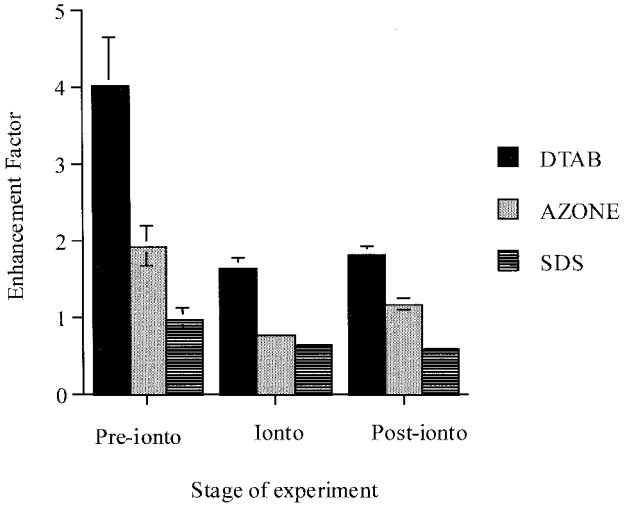

Fig. 3. Effect of chemical and iontophoretic treatment on D-CB delivery across human SC. Enhancement factors (EFs) were determined by dividing the appropriate J_{ss} following given enhancer treatment by the corresponding J_{ss} following neat PG treatment.

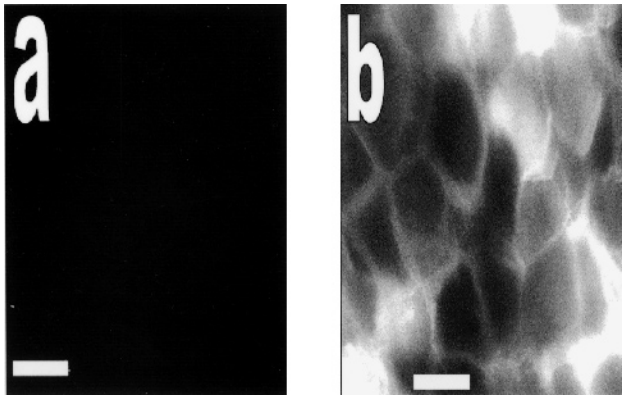

Fig. 4. TPEM XY images (95 × 95 μm^2) showing passive D-CB transport across human stratum corneum. The figure shows a depth of 10 μm after 60 minutes of drug application: (a) untreated skin and (b) following pretreatment with 0.16 M DTAB. The scale bar represents 20 μm.

resulting D-CB flux depended upon the enhancer; J_{ss} increased by a factor of at least 10, relative to the corresponding passive fluxes and that DTAB pretreatment coupled with iontophoresis achieved the highest absolute D-CB flux (477 ± 29.3 ng cm^{-2} h^{-1}) of all the treatment protocols described (Table I). In contrast, Azone® and SDS markedly attenuated flux during iontophoresis ($p < 0.05$). Furthermore, PG pretreatment prior to iontophoresis offered no additional benefit compared to the iontophoresis-alone protocol.

The dependence of the enhancement on permeant molecular weight was assessed for the enhancer, Azone® by investigating the influence of Azone®/PG on the transport of the anionic label Cascade Blue® (CB; $M_R = 548$ Da). The resulting permeation profiles, and steady-state fluxes are shown in Fig. 5 and Table I. As with D-CB, passive transport of CB across untreated skin was below the analytical limit of detection but was greatly enhanced by all treatment regimens. Additionally, the data show that the passive (following PG pretreatment) and iontophoretic transport of this smaller anion was significantly elevated ($p > 0.05$) relative to the delivery of D-CB, under identical experimental conditions. In contrast, the passive transport of CB following Azone® pretreatment, is not significantly ($p < 0.05$) different to that of the larger anion, D-CB, despite a 6-fold difference in molecular weight. Moreover, as with D-CB transport, the combined application of Azone®/PG and iontophoresis significantly decreases the delivery of CB relative to the corresponding regimen without Azone®.

These results demonstrate that (a) pretreatment with cationic DTAB, of the chemical enhancers tested, produces the greatest enhancement of passive D-CB transport; (b) DTAB pretreatment coupled with iontophoresis achieves the highest absolute D-CB flux of all the treatment protocols described; (c) the enhancing ability of iontophoresis combined with chemical pretreatment is not greater than the sum of the effects of iontophoresis or chemical pretreatment employed individually—i.e., there is no evidence of synergism between the two enhancement regimens; (d) the dual application of chemical pretreatment (Azone® or SDS) and iontophoresis can attenuate the iontophoretic driving force for D-CB transport; and (e) this latter phenomenon is also observed for the iontophoretic delivery of the smaller anion, CB, following Azone® pretreatment.

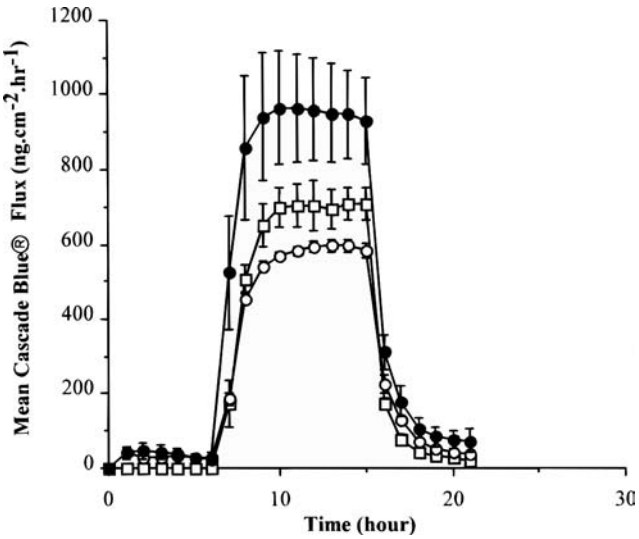

Fig. 5. Passive and iontophoretic permeation profiles of free Cascade Blue® (0.1 mM) across human stratum corneum. —□—, untreated SC; —○—, pretreatment with 0.16 M Azone® in PG; —●—, neat propylene glycol. Current was applied for nine hours between t = 6 and t = 15 h.

The application of an iontophoretic driving force (at constant current) might be expected to enhance the delivery of D-CB from all systems with, perhaps, enhancer pretreatment further increasing flux. A possible basis of enhancer selectivity is an interaction between the relative charges of the membrane, permeant, enhancer and driving electrode. The permselective nature of the skin, conferred by its net negative charge at physiological pH (28), favours the transport of neutral and positively charged permeants in the anode-to-cathode direction (29); the cathodal transport of D-CB is, thus, already compromised. Pretreatment with chemical enhancers may offer a means to modify this membrane permselectivity and, indeed, the modulation of skin permselectivity has recently been the subject of considerable investigation (6–9). Although electroosmotic and electrorepulsive contributions to D-CB iontophoretic flux cannot be isolated here, it is likely that the positively-charged enhancer, DTAB, interacts with the negative charge of the skin and facilitates cathodal delivery of anionic D-CB across a membrane which reduced discrimination against anions (477.2 ± 29.3 ng cm^{-2} h^{-1}). In contrast, the negatively-charged SDS may augment surface negativity and, hence, retard the cathodal transport of D-CB (172.7 ± 7.0 ng cm^{-2} h^{-1}) or else SDS anions may compete with D-CB anions during cathodal iontophoresis (8). Additionally, SDS may be repelled at the cathode, driving it from the SC and attenuating its effect while DTAB may be retained at the cathodal surface to prolong its effect. The neutral enhancers provide reference fluxes between these extremes with Azone® (210.3 ± 9.6 ng cm^{-2} h^{-1}) being of the same order as PG (272.7 ± 17.0 ng cm^{-2} h^{-1}).

The iontophoretic transport of D-CB was also visualised in human epidermis (split-thickness skin, 200 μm section) to assess penetration into deeper skin layers. The iontophoretic D-CB flux across this skin was 496 ± 14.4 ng cm^{-2} h^{-1}—a value not statistically different ($p > 0.05$) to that across isolated SC (477.2 ± 29.3 ng cm^{-2} h^{-1}). Consequently, the SC distribution of D-CB fluorescence intensity seen in split-thickness skin was representative of that in isolated SC and, thus, allowed comparison with permeation profiles obtained using SC membranes. Figure 6a shows a typical series of TPE images (in the XY plane) taken at three different depths in SC at varying time points during the iontophoretic delivery of D-CB after pretreatment with DTAB/PG. Control experiments revealed negligible autofluorescence arising from skin tissue. In all series, average fluorescence intensity decreased with increasing depth. The first set of images obtained (at 10 μm) show, initially, a predominant intercellular distribution of D-CB—corneocyte cell contours are clearly defined. As iontophoresis proceeds, the label intensity increases strongly in certain regions. Images after 60 and 120 minutes of iontophoresis show that these regions correspond with the shape of cells, indicating a significant amount of D-CB uptake into corneocytes. This may be a consequence of surfactant-induced swelling (30) as DTAB penetrates the SC and resulting in enhanced corneocyte membrane permeability. Alternatively, this penetration could lower cell negativity, ensuing in a greater affinity for D-CB. Deeper

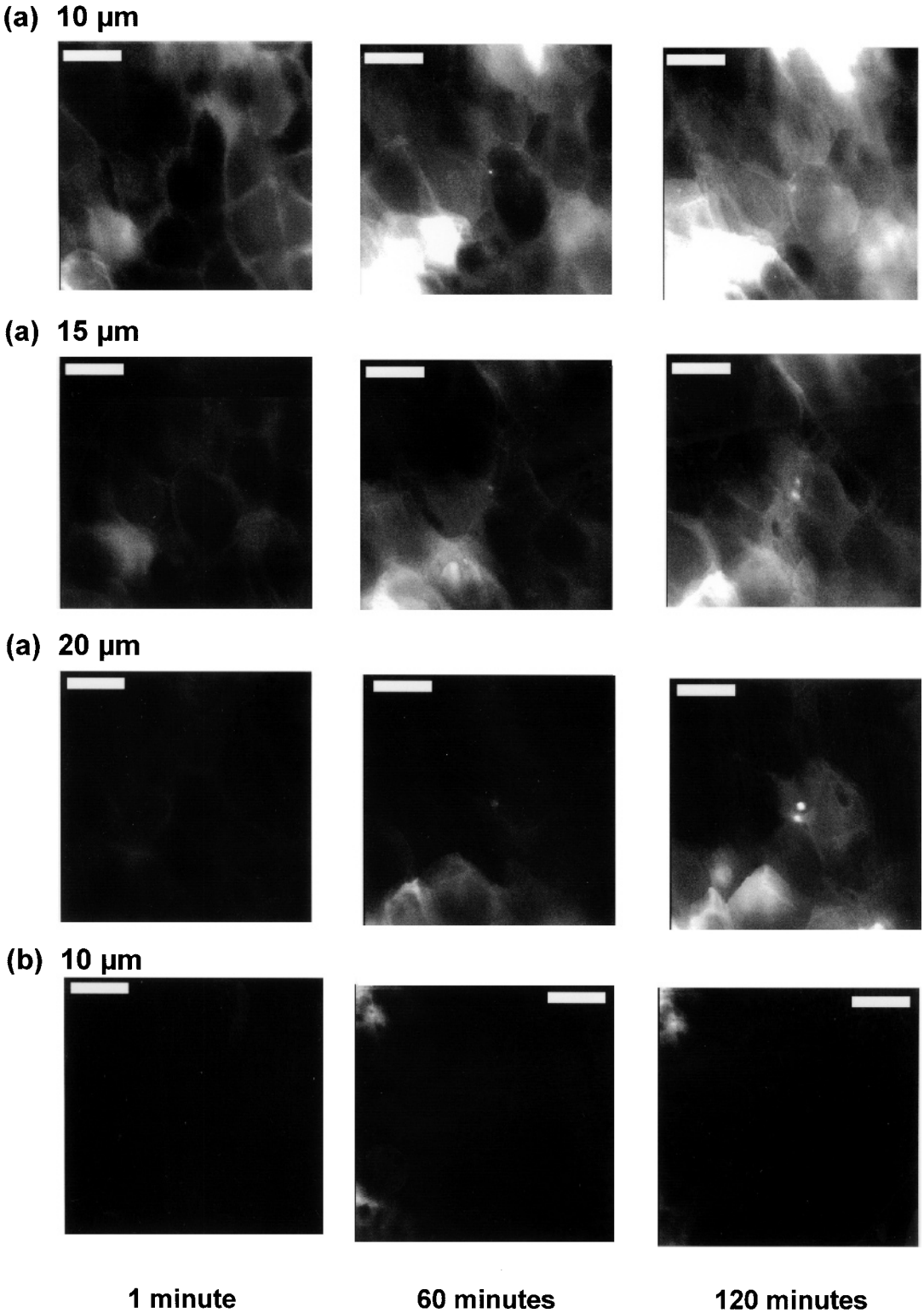

Fig. 6. TPEM XY images (95 × 95 μm^2) showing D-CB transport across human stratum corneum as a function of time and depth, during iontophoresis. (a) pretreatment with DTAB in PG; (b) untreated human stratum corneum; all images are scaled to the same intensity. The scale bar represents 20 μm.

into the membrane, D-CB also shows both an inter- and intracellular distribution. Control images of untreated skin after equivalent scaling (see Fig. 6b) exhibited visible label intensity only at a depth of 10 μm in SC and was at least an order of magnitude less in intensity than the images shown. At depths of 15 and 20 μm, samples, after iontophoresis without DTAB pretreatment, exhibited negligible D-CB distribution. Comparison of Fig. 4b (passive diffusion across DTAB treated SC) and Fig. 6b (iontophoretic transport across untreated SC) at a depth of 10 μm show a greater fluorescent intensity in the former images, in contrast to a higher measured flux during the iontophoretic protocol.

These data are consistent with a significant appendageal contribution to iontophoretic transport (12). Other studies have reported the follicular distribution of positively charged, fluorescently labelled macromolecules of similar molecular weight to D-CB following cutaneous iontophoresis (16). This appendageal distribution was more noticeable at depths ranging from 20–40 μm into skin while, at more superficial depths, significant non-follicular distribution was evident. However, due to the high magnifications used in the present study, it was not possible to simultaneously visualise possible transport in skin appendages. Whether this transport route is also of importance for anionic macromolecules warrants further TPEM investigations at lower magnifications.

Figure 7 is a series of images obtained in the XZ plane (perpendicular to the skin surface) of a sample showing D-CB transport into DTAB/PG pretreated skin. The white band at the base of each image represents the D-CB applied to the skin. The SC is the visible cellular layer (10–20 μm) above and adjacent to this band. Following the application of current (Fig. 7b and 7c), the SC becomes less well defined, as D-CB is transported across it and deeper into the split-thickness skin. TPEM imaging is clearly able to show dextran transport up to 80 μm deep in the split-thickness skin. From the skin samples examined, substantially enhanced iontophoretic macromolecular transport was visualised. However, the pattern of distribution visualised by XZ-imaging was variable, when comparing different samples, reflecting the heterogeneity of the tissue; transport most likely taking the route of least resistance in each sample.

Post-Iontophoresis

After the termination of current, D-CB flux values declined rapidly and reached steady-state approximately 3 hours after current cessation. With the exception of the DTAB treatment, the passive J_{ss} values (Table I) remained significantly greater than those measured passively prior to current application ($p < 0.05$). Indeed, the data suggest that DTAB treatment perturbs the SC barrier more than does current application.

Size-Exclusion Chromatography

The possibility exists that the D-CB was polydisperse and (i) the SC could behave permselectively, favouring the diffusion of smaller dextran fragments and hence affect true flux or (ii) free label was dissociated from the macromolecule during transport. SEC was used to assess the characteristics of transported dextran. The size-exclusion chromatograms of solutions in different cell compartments during transport studies (not shown) indicate a single peak for D-CB (t_R 7.81 min) and for CB (t_R 9.3 min). D-CB in the receiver solutions was identical to that in the donor and negligible levels of free label were detected showing that the SC was not behaving permselectively and that dextrans were not being degraded in the SC nor indeed by the application of current. Dextran structural integrity was shown to be maintained throughout experimental lifetime and the chromatograms indicate that the D-CB content of donor and receptor compartments was not bound to membrane and/or formulation constituents, nor existed as irreversible ion-pairs (e.g., with DTAB).

CONCLUSIONS

The ability of transdermal enhancers to modulate the passive and iontophoretic delivery of a model, anionic macromolecule (M_R = 3 kDa) has been demonstrated. The separate application of DTAB, SDS, Azone® and iontophoresis improved the cutaneous delivery of D-CB but the efficiency of a combined chemical and iontophoretic approach was dependent upon the relative charges of the permeant, enhancer and driving electrode. Real-time analysis provided visual verification of DTAB- and DTAB/iontophoretically-enhanced D-CB transport across human SC. Passive transport following DTAB pretreatment was characterised by significant intercellular D-CB distribution; the supplementary application of a current also resulted in intracellular uptake. To the best of our knowledge, this is the first study to report the on-line visualisation, using TPEM, of iontophoretic transport across human skin. This methodology offers distinct advantages over conventional techniques, enabling the dynamic

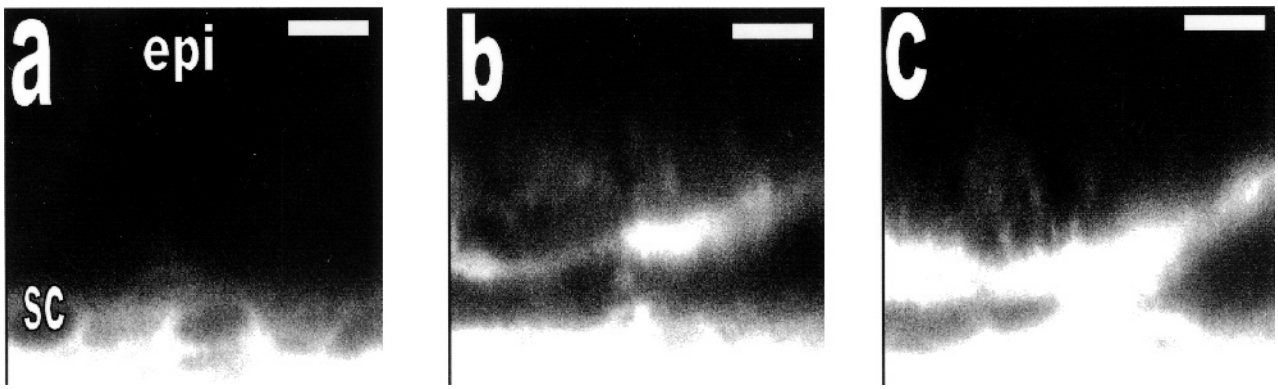

Fig. 7. TPEM XZ images (95 × 95 μm^2) showing D-CB transport through DTAB/PG pretreated human epidermis (split-thickness skin) during passive and iontophoretic delivery at various time points. Treatments are: (a) 1 hour passive, (b) 1 hour of iontophoresis, (c) 2 hours of iontophoresis; SC, stratum corneum; epi, epidermis. The scale bar represents 20 μm.

visualisation of transport, and consequently, rapid differentiation between transport pathways and static regions of penetrant accumulation which have a high affinity for the permeant which is exaggerated by virtue of the time-lag between sample preparation and visualisation.

ACKNOWLEDGMENTS

We thank the Aston Pharmacy School and The James Watt Memorial Foundation for financial support.

REFERENCES

1. E. W. Smith and H. I. Maibach. *Percutaneous Penetration Enhancers*, CRC Press, Boca Raton, 1995.
2. B. J. Aungst, N. J. Rogers, and E. Sheffer. Enhancement of Naloxone penetration through human skin in vitro using fatty acids, fatty alcohols, surfactants, sulfoxides and amides. *Int. J. Pharm.* **33**:225–234 (1986).
3. J. A. Bouwstra, G. S. Gooris, J. Brussee, M. A. Salomons-de Vries, and W. Bras. The influence of alkyl-azones on the ordering of the lamellae in human stratum corneum. *Int. J. Pharm.* **79**:141–148 (1992).
4. P. K. Wotton, B. Møllgaard, J. Hadgraft, and A. Hoelgaard. Vehicle effect on topical drug delivery. III. Effect of Azone on the cutaneous permeation of metronidazole and propylene glycol. *Int. J. Pharm.* **24**:19–26 (1985).
5. A. Naik, L. A. R. M. Pechtold, R. O. Potts, and R. H. Guy. Mechanism of oleic acid induced skin penetration enhancement. *J. Contr. Rel.* **37**:299–306 (1995).
6. J.-Y. Fang, C.-L. Fang, Y.-B. Huang, and Y.-H. Tsai. Transdermal iontophoresis of sodium nonivamide acetate. III. Combined effect of pretreatment by penetration enhancers. *Int. J. Pharm.* **149**:183–193 (1997).
7. J. Hirvonen, K. Kontturi, L. Murtomaki, P. Paronen, and A. Urrti. Transdermal Iontophoresis of Sotalol and Salicylate; the effect of skin charge and penetration enhancers *J. Contr. Rel.* **26**:109–117 (1993).
8. C. L. Gay, P. G. Green, and M. L. Francoeur. Iontophoretic delivery of piroxicam across the skin in vitro. *J. Contr. Rel.* **22**:57–68 (1992).
9. L. Wearley and Y. W. Chien. Enhancement of the in vitro skin permeability of Azidothymidine (AZT) via iontophoresis and chemical enhancer *Pharm. Res.* **7**:34–40 (1990).
10. N. Yoshida and M. Roberts. Solute molecular size and transdermal iontophoresis across excised human skin. *J. Contr. Rel.* **25**:177–195 (1993).
11. P. G. Green, B. Shroot, F. Bernerd, W. R. Pilgrim, and R. H. Guy. In vitro and in vivo iontophoresis of a tripeptide across nude rat skin. *J. Contr. Rel.* **20**:209–218 (1992).
12. P. G. Green, M. Flanagan, B. Shroot, and R. H. Guy. Iontophoretic Drug Delivery. In K. A. Walters and J. Hadgraft (eds), *Pharmaceutical Skin Penetration Enhancement*, Marcel Dekker Inc, New York, 1993, pp. 311–333.
13. B. Berner and S. M. Dinh. Electronically assisted drug delivery: An overview. In B. Berner and S. M. Dinh (eds), *Electronically controlled drug delivery*, CRC Press, New York, 1998, pp. 3–7.
14. C. Cullander and R. H. Guy. Visualization of iontophoretic pathways with confocal microscopy and the vibrating probe electrode. *Solid-state Ionics* **53**:197–206 (1992).
15. N. G. Turner and R. H. Guy. Iontophoretic transport pathways: Dependance on penetrant physicochemical properties. *J. Pharm. Sci.* **86**:1385–1389 (1997).
16. N. G. Turner, L. Ferry, M. Price, C. Cullander, and R. H. Guy. Iontophoresis of Poly-L-lysines: The role of molecular weight? *Pharm. Res.* **14**:1322–1331 (1997).
17. J. Vroom. Two-photon excitation fluorescence lifetime imaging: development and biological applications. PhD Thesis, Universiteit Utrecht, Faculteit Natuur-en Sterrenkunde, pp. 1–93 (1998).
18. C. Cullander, Confocal microscopy in the study of skin permeation: Utility and limitations. In K. A. Walters, K. Brain and V. J. James (eds), *Prediction of Percutaneous Penetration*, STS Publishing, Cardiff, 1996, pp. 5–6.
19. K. König P. T. C. So, W. W. Mantulin, and E. Gratton. Cellular response to near-infrared femtosecond laser pulses in two-photon microscopes. *Optics Letts.* **22**:135–136 (1997).
20. L. A. Geddes, L. E. Baker, and A. G. Moore. Optimum electrolytic chloriding of silver electrodes. *Med. Biol. Eng.* **7**:49–56 (1969).
21. R. Van der Geest, M. Danhof, and H. E. Boddé. Validation and testing of a new iontophoretic continuous flow through transport cell. *J. Contr. Rel.* **51**:85–91 (1998).
22. C. J. de Grauw, J. M. Vroom, H. T. M. van der Voort, and H. C. Gerritsen. Imaging properties of in two-photon excitation microscropy and effects of refractive index mismatch in thick specimens, *Applied Optics* **38**:5995–6003 (1999).
23. N. M. Volpato, P. Santi, and P. Colombo. Iontophoresis enhances the transport of acyclovir through nude mouse skin by electrorepulsion and electroosmosis. *Pharm. Res.* **12**:1623–1626 (1995).
24. J. A. Bouwstra and H. E. Bodde, Human SC barrier impairment by N-alkyl-azacycloheptanones: A mechanistic study of drug flux enhancement, Azone mobility, and protein- and lipid-perturbation. In: *Percutaneous Penetration Enhancers*, E. W. Smith, and H. I. Maibach (eds.), New York: CRC Press, pp. 137–157, (1995).
25. Y. N. Kalia and R. H. Guy, The interaction between penetration enhancers and iontophoresis: Effect on human skin impedance *in vivo*, *J. Contr. Rel.* **44**:33–42 (1997).
26. P. Ashton, K. A. Walters, K. R. Brain, and J. Hadgraft. Surfactant effects in percutaneous absorption I. Effects on the transdermal flux of methyl nicotinate. *Int. J. Pharm.* **87**:261–264 (1992).
27. J. Hadgraft, D. G. Williams, and G. Allan. Azone®, Mechanisms of action and clinical effect. In K. A. Walters and J. Hadgraft (eds), *Pharmaceutical Skin Penetration Enhancement*, Marcel Dekker, New York, 1993,
28. R. R. Burnette and B. Ongpipattanakul. Characterization of the permselective properties of excised human skin during iontophoresis. *J. Pharm. Sci.* **76**:765–773 (1987).
29. A. Kim, P. G. Green, G. Rao, and R. H. Guy. Convective solvent flow across the skin during iontophoresis. *Pharm. Res.* **10**:1315–1320 (1993).
30. L. D. Rhein, C. R. Robbins, K. Fernee, and R. Cantore. Surfactant structure effects on swelling of isolated human stratum corneum. *J. Soc. Cosmet. Chem.* **37**:125 (1986).